

Photochemistry of Halide Ion–Molecule Clusters: Dipole-Bound Excited States and the Case for Asymmetric Solvation

CAROLINE E. H. DESSENT, JUN KIM, AND MARK A. JOHNSON*

Sterling Chemistry Laboratory, Yale University, P.O. Box 208107, New Haven, Connecticut 05620

Received October 20, 1997

I. Introduction

One of the most elementary aspects of chemistry is the dissolution of salts into independently solvated ions. Virtually all introductory chemistry textbooks discuss the phenomenon in the context of the formation of shells of solvent molecules around these ions. Our focus here is on the nature of halide anions, X^- , in the presence of the first few solvent molecules, M , isolated in a gas-phase cluster ion, $X^- \cdot M_n$. Such clusters allow us to directly explore the solvent exposed to the extreme electric fields in the vicinity of the ion where the dielectric response is thought to be saturated.¹ While one might suspect that such clusters form by sequentially filling up the first solvent shell, recent results from our laboratory lead to some surprising conclusions^{2,3} regarding how polar solvent molecules arrange themselves in the primary steps of solvation. In this paper, we present the photochemical strategy specifically developed to attack the problem of solvation morphology and discuss the disposition of the first two solvent molecules. In addition, we point out an unexpected spin off from this work, where the photochemistry of the anions suggests an efficient photosynthetic preparation scheme for rare isomers of neutral van der Waals complexes.

To set the stage, consider the case of a polar solvent, where dielectric saturation arises primarily due to orientational locking of the molecules in the inner coordination

shell. Acetonitrile is an archetypal example of a polar solvent with its large molecular electric dipole moment ($\mu = 3.92$ D). Calculations⁴ indicate that the potential minimum of the binary $X^- \cdot CH_3CN$ “ion–dipole complex” occurs for the linear arrangement, with the ion bound to the electropositive methyl “pocket”. Intuitively, one might suspect that the placement of the second solvent molecule is similarly obvious. If both molecules reside close to the ion, sequentially building up the solvation shell, then the dipoles will both be aligned with positive ends toward the ion and therefore repel one another. Minimization of this repulsion therefore leads to an arrangement in which the solvent molecules are antiparallel, located on opposite poles of the ion. There are alternative structures, however, such as one where the solvent molecules are bound together (i.e. end-to-end) to form a linear van der Waals complex with a very high net dipole moment⁵ which then binds to the ion. Thus, we envision the two extreme cases illustrated in Chart 1.

Chart 1



While the asymmetric structure places the second molecule in what will ultimately become the second solvation shell, we will show that this form is indeed generally adopted for high symmetry (i.e. C_{3v}) dipolar solvent molecules. We begin this discussion by reviewing the recent advances in the photophysics of ion–molecule complexes which lead us to this surprising conclusion.

II. Dipole-Bound Excited States of Anion–Molecule Complexes and “Photosynthesis” of Dipole-Bound Anions

IIA. Excess Electrons and Dipole-Bound States. Typical solvents (water, acetonitrile, acetone, etc.) are clear liquids composed of closed shell molecules whose first electronically excited states lie well into the ultraviolet region of the spectrum. This is, of course, a highly desirable property for a solvent since it provides for chemically inert media in which to conduct reactions. The neutral LUMOs of such molecules are therefore high in energy, and the valence anions (M^-) formed by occupation of the LUMOs spontaneously eject (autodetach) an electron back into the continuum. Such unstable valence anions are called resonances or transient negative ions⁶ and can only be observed by electron scattering or via the photon energy dependence of the negative ion photoelectron spectrum.⁷ On the other hand, if the dipole moment, μ , of the closed shell neutral molecule is above a critical value^{8,9} of about 2 D, a low-energy, so-called “excess” electron can become trapped *outside* the molecular orbital network by the long-range electrostatic field of the neutral. These states are very weakly bound (~ 10 meV) with extremely diffuse orbitals (~ 30 Å).¹⁰ With increasing cluster size, this effect evolves into bulk “solvated electrons”, the most famous of which is certainly that formed in metal–ammonia

Caroline E. H. Dessent received her M.A. from Jesus College, Oxford University, in 1991 and obtained her Ph.D. from Yale University in 1997 for work on dipole-bound excited states with Mark Johnson. She is currently a research fellow at the University of York, working on the dynamics of molecular clusters with Klaus Müller-Dethlefs.

Jun Kim received his B.A. degree in chemistry from Franklin and Marshall College (1994) and is currently a Ph.D. candidate at Yale University. His research interests involve following the ultrafast kinetics of reactions in clusters.

Mark A. Johnson received his B.S. degree in chemistry from the University of California at Berkeley (1977) and his Ph.D. from Stanford (1983). After working as a postdoctoral associate at JILA (1983–1985), he joined the faculty at Yale where he is currently professor of chemistry. His interests are in the elucidation of solvent effects in chemistry through the study of size-selected clusters.

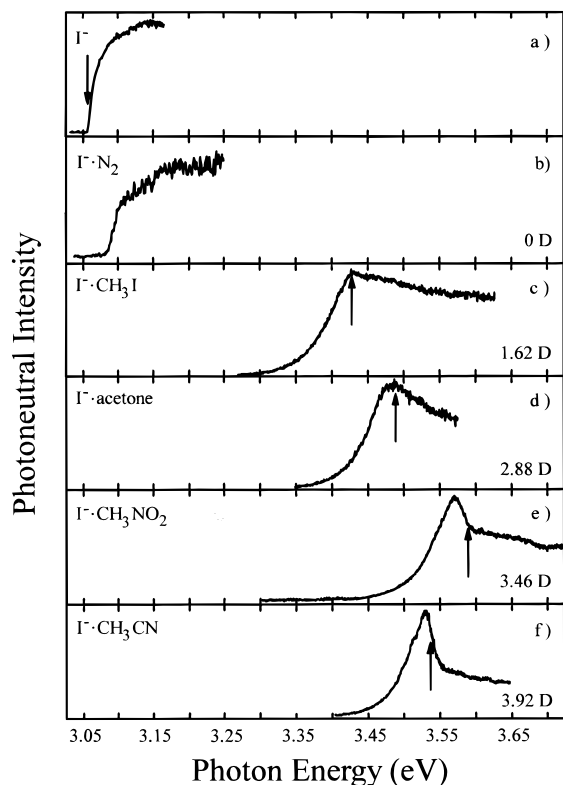


FIGURE 1. Absorption (fast photoneutral action) spectra of (a) the I^- ion and (b–f) $\text{I}^- \cdot \text{M}$ ion–molecule complexes. Arrows indicate the positions of the vertical detachment energies of the I^- ion and the $\text{I}^- \cdot \text{M}$ complexes. Electric dipole moments for various solvents are included in the lower right of each panel.

solutions,¹¹ where their characteristic blue color arises from “free” electrons trapped within cavities in the structure of the liquid.¹²

A solvent molecule’s ability to trap an excess electron is key to our method. Consider the electronic absorption spectrum of an isolated halide ion, such as I^- . The I^- absorption spectrum is shown at the top of Figure 1, beginning promptly at the electron affinity with a sloping onset corresponding to a “Wigner” threshold law.¹³ Unlike neutral species, with their associated dense manifolds of Rydberg states just below each ionization threshold, atomic anions typically do not possess *any* bound excited electronic states (only the excited resonances mentioned earlier), and therefore the first absorption often occurs directly to the continuum:



This situation changes dramatically, however, when a single solvent molecule, M, is complexed with the halide, since a highly dipolar solvent molecule can itself support a bound state of the ion–molecule complex, provided $\mu_{\text{M}} > 2\text{D}$. This state, based on the dipole-bound ground-state ion, M^- , then becomes the first excited state of the cluster:



Note that M^- in eq 2 is meant to indicate that the electron is trapped by the dipole moment of M, and we caution

that this notation is somewhat misleading since the electron is actually far from M. In fact, the dipole-bound orbital¹⁴ is largely displaced beyond the halogen atom, away from M rather than toward it.

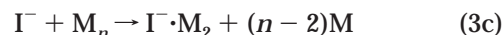
II B. Some Experimental Details. Cluster ions, $\text{I}^- \cdot \text{M}_n$ ($n = 1, 2$) are prepared by ionization at the throat of a supersonic expansion containing the ambient vapor pressure of a mixture of methyl iodide and the relevant solvent in 2–3 atm of argon. The clusters are formed in a two-step process,¹⁵ involving production of the iodide ion via dissociative electron attachment onto methyl iodide



followed by three-body association onto the solvent molecule, M,

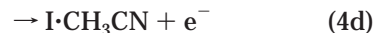


or by direct condensation with a neutral cluster,



Reactions 3b and 3c proceed in a relatively high-density region of the expansion,¹⁵ allowing some cooling of the ion–molecule complexes as they drift ~ 15 cm before being pulsed into the mass spectrometer. The clusters are then mass selected by time-of-flight prior to being analyzed in the photofragmentation spectrometer.¹⁵

Photofragmentation action spectra of the iodide clusters were scanned over the region of their electron detachment thresholds, determined using negative ion photoelectron spectroscopy.¹⁶ Action spectra were acquired for both anionic fragments and (fast) “photoneutrals”. The utility of the latter is that, for an electronically excited complex such as $\text{I}^- \cdot \text{CH}_3\text{CN}$, we can imagine a variety of decomposition pathways:



where all channels lead to production of a fast neutral partner possessing typically 2 keV kinetic energy (from the fast ion beam), which is easily detected using a micro-channel plate secondary electron multiplier. Thus, the photoneutral spectra do not discriminate between decay channels and are most similar to photodestruction spectra of the ion beam. In the absence of fluorescence (which can regenerate the ground-state cluster ion), photodestruction is equivalent to absorption, and we regard the photoneutral spectra as being largely equivalent to absorption. The fast neutrals were detected after deflecting all charged particles away from the beam, while the photofragment ions were isolated using a tandem time-of-flight spectrometer.¹⁵ The UV photons necessary to detach the high-electron affinity iodide ion–molecule

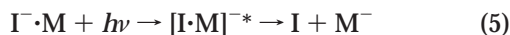
complexes were generated by a broadly tunable optical parametric oscillator (OPO). The OPO output was either summed with the fundamental to produce 3.35–3.70 eV photons or frequency doubled to generate 3.70–4.20 eV photons.

III. $I^- \cdot M$ Binary Complexes

IIIA. Electronic Spectra of the $I^- \cdot M$ Binary Complexes.

To explore the influence of a solvent molecule on the I^- electronic chromophore, we display in Figure 1 the photoneutral action spectra for several $I^- \cdot M$ complexes, where M has a sequentially increasing dipole moment. The arrows represent the so-called vertical electron detachment energies (VDEs) of the complexes (obtained from the negative ion photoelectron spectra^{16–22}), corresponding to the electron binding energies with the complexes frozen at the equilibrium geometries of the anions. Solvation of the iodide ion by a nitrogen molecule (Figure 1b) leaves the absorption spectrum largely unchanged, but the bare I^- profile is significantly perturbed when the halide ion is solvated by a polar molecule (Figure 1c–f), with the onset becoming much more gradual. Most noticeably, an absorption maximum develops just below the VDE, before the spectrum smoothly tails off toward higher photon energies. The prominence of this maximum evolves with the dipole moment of the solvent molecule, developing into a clear peak *below* the VDE in the $I^- \cdot CH_3NO_2$ and $I^- \cdot CH_3CN$ complexes.

IIIB. Photoproduction of Dipole-Bound Solvent Anions. To probe the nature of the excited-state evident in the $I^- \cdot CH_3NO_2$ and $I^- \cdot CH_3CN$ absorption spectra (Figure 1e,f), the ionic photofragments produced at each maximum were dispersed in a reflectron secondary mass analyzer. The photofragment mass spectrum from $I^- \cdot CH_3CN$, for example, reveals that the only ionic photofragment is CH_3CN^- —a known dipole-bound, ground-state anion.²³ Note that photoexcitation has effectively cleaved the solvent molecule from the halide ion—this property will be exploited in our synthesis of van der Waals isomers in section IV. The action spectra for production of the CH_3CN^- and $CH_3NO_2^-$ anions upon photoexcitation of $I^- \cdot CH_3CN$ and $I^- \cdot CH_3NO_2$, respectively, are shown by the dashed lines in Figure 2. In each case, the peak in the absorption spectrum results from excitation to a state which decays by fragmentation into the corresponding dipole-bound anion, M^- :



The fragmentation of the excited states into dipole-bound anions implies that the excited states also possess diffuse excess electrons. Since the peaks in the absorption spectra evolve as a function of solvent molecule's dipole moment, they are assigned as excitations to dipole-bound excited states of the ion–molecule complexes.

IIIC. Characterization of the Dipole-Bound Anions of Single Solvent Molecules. It is worthwhile emphasizing that this photochemical method (eq 5) is an extremely efficient synthetic route to the delicate²⁴ ground-state,

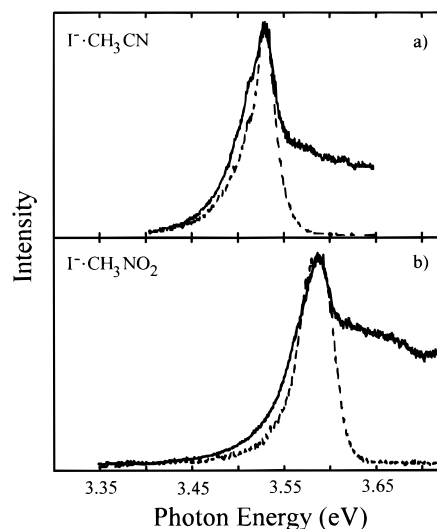


FIGURE 2. Overlay of the absorption (solid lines) and photofragmentation action spectra (dashed lines) from (a) $I^- \cdot CH_3CN$ and (b) $I^- \cdot CH_3NO_2$. The dashed lines are the action spectra for production of the CH_3CN^- and $CH_3NO_2^-$ dipole-bound photofragment ions in a and b, respectively.

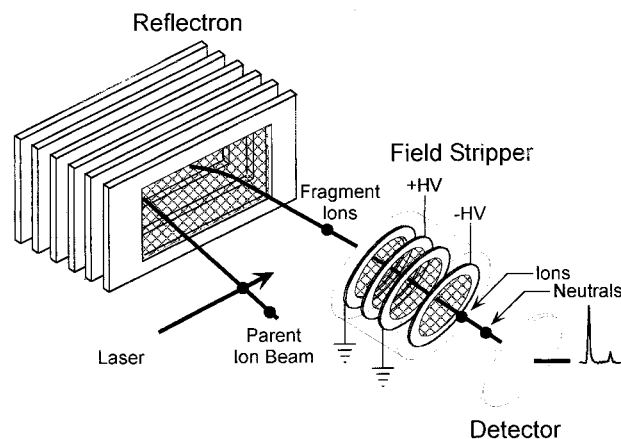


FIGURE 3. Illustration of the experimental apparatus used to field-detach excess electrons from photogenerated dipole-bound anions, consisting of three equally spaced (0.30 cm) grids, which are oriented perpendicular to the ion beam axis. The outer grids are grounded while a positive voltage (0–10 kV) is applied to the central grid. A fourth grid placed after this arrangement can be negatively biased, which allows fast neutrals to be completely isolated from the parent ions.

dipole-bound anions as more than 50% of the intense parent cluster ion can be converted to the dipole-bound photofragment ion. For example, using this method we were able to conduct the first spectroscopic characterization⁷ of an isolated ground-state, dipole-bound anion, CH_3CN^- , by photoelectron spectroscopy. However, there is a simpler test for identifying a diffuse, dipole-bound electron, which involves charge stripping with a moderate electric field.²⁵ The CH_3CN^- photofragment was therefore subjected to an electric field generated with the apparatus depicted in Figure 3. The raw data from a stripping experiment are presented in Figure 4a, which displays the arrival time spectra on a detector placed at the output of the high-field region. The upper trace consists of just the CH_3CN^- anion peak at zero field. As the field is increased,

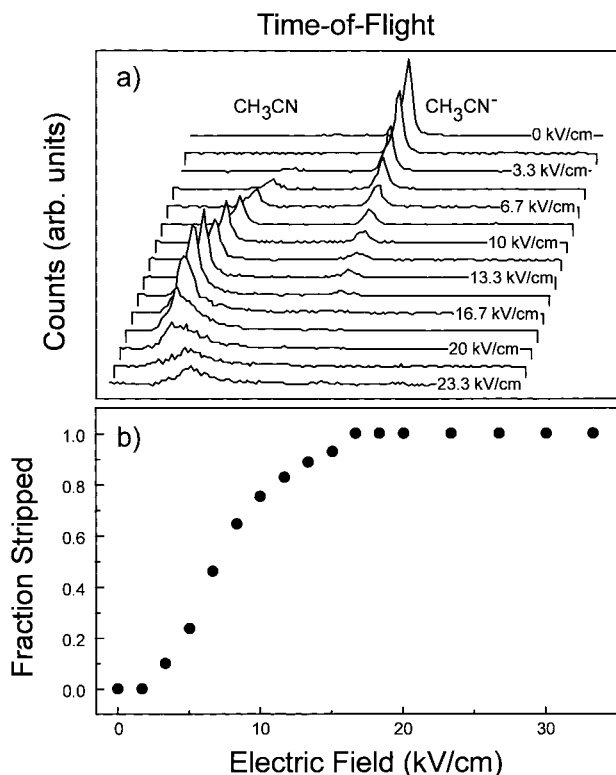


FIGURE 4. (a) Time-of-flight spectra of the dipole-bound CH_3CN^- photofragment anion at various electric fields. As the field increases, a new peak grows in corresponding to the formation of the CH_3CN neutral. (b) Plot of the fraction of neutrals produced by stripping the weakly bound electron from the CH_3CN^- anion as a function of field strength.

a new peak grows in corresponding to the stripped CH_3CN neutral, which appears at shorter time since the ion is accelerated before the electron falls off with a unimolecular rate, $k(\mathcal{E})$:



where $k(\mathcal{E})$ is a strongly increasing function of electric field, \mathcal{E} . As the field is increased above 10 kV, the ion strips earlier in the high-field region, and the neutral acquires less kinetic energy and hence arrives closer to the parent ion. Note that the fast neutral peak is indeed about the same magnitude as that of the parent ion, indicating that the detection efficiencies of ions and fast neutrals are similar. Figure 4b presents the stripping efficiency (i.e. fraction of anions stripped at each field value). We will return to field detachment in section IV as it proves to be a promising technique for the final step in our synthesis of van der Waals isomers. We first review the photophysics of dipole-bound excited states; more casual readers may wish to proceed directly to section IV to continue the discussion of anionic solvation.

III.D. Remarks on the Photofragmentation Mechanism. It is useful to consider the decay mechanism of a dipole-bound excited state which leads to ejection of the neutral iodine atom (eq 5). Since the interatomic force field describing diffuse dipole-bound excited states is largely that of the neutral core, we can infer the ionic

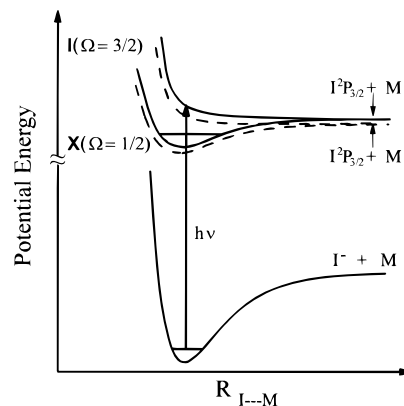


FIGURE 5. Schematic diagram illustrating the two surfaces, \mathbf{X} ($\Omega = 1/2$) and \mathbf{I} ($\Omega = 3/2$), of the neutral $\text{I}\cdot\text{M}$ complex accessed in photodetachment of the $\text{I}^-\cdot\text{M}$ ion-molecule cluster (over the lower energy, $^2\text{P}_{3/2}$, spin-orbit state of the iodine atom). The dashed lines represent the dipole-bound excited states of the anionic complex that are built on these neutral states.

photophysics from that of the neutral complexes formed in photodetachment. The $\text{I}\cdot\text{M}$ neutral clusters have been studied by Neumark and co-workers^{22,26} using very high-resolution zero electron kinetic energy (ZEKE) spectroscopy of anions such as $\text{I}^-\cdot\text{Ar}$. The ZEKE spectra reveal two low-lying electronic states of the neutral complex, \mathbf{X} and \mathbf{I} , derived from the lower energy $^2\text{P}_{3/2}$ spin-orbit state of the halogen. Qualitatively, these arise from the different (Σ , Π) orientations of the p-electron in the radical atom relative to the molecular axis of M . The upper state, \mathbf{I} , is a Π state (in cylindrical symmetry) with the lone pair oriented toward M , and is often repulsive over the geometry of the ground-state complex. This was particularly evident in the $\text{I}\cdot\text{CH}_3\text{I}$ complex,²² where bound (i.e. vibrational) structure was only found in the \mathbf{X} state.

When the dipole moment of M is larger than the critical value (~ 2 D), one dipole-bound anionic excited state should be associated with each of the neutral states, as depicted by the dashed lines in Figure 5. We therefore expect that the first excited anionic state is often built on a repulsive neutral core. This repulsive state produces the dipole-bound solvent anions since the ejected neutral iodine atom is ineffective at retrapping the diffuse electron into its atomic orbitals²⁷ to re-form I^- , leaving the delocalized electron dipole-bound to the polar solvent molecule as the core dissociates. These photophysics are fundamentally equivalent to a half-collision analogue of the Rydberg electron-transfer method of preparing ground-state, dipole-bound anions [$\text{RG}^{**} + \text{CH}_3\text{CN} \rightarrow \text{CH}_3\text{CN}^- + \text{RG}^+$ ($\text{RG} = \text{rare gas}$)], first demonstrated by Compton in 1974.²⁸

III.E. Qualitative Interpretation of the Absorption Profiles. The assignment of the prethreshold peak in the $\text{I}^-\cdot\text{M}$ absorption spectra to a diffuse, dipole-bound excited state nicely explains the qualitative evolution of the peak intensity with increasing dipole moment of M (Figure 1). Recall that the optical absorption cross section, $\sigma(h\nu)$, is generally governed by the transition dipole matrix element:

$$\sigma(h\nu) \propto \langle \phi_g(r) | r | \phi_f^E(r) \rangle^2 \quad (7)$$

between the ground-state orbital, $\phi_g(r)$, from which the electron is ejected and the final state (one electron) wave function, $\phi_f^E(r)$, which is either a bound or continuum state at energy, E . In the present case, $\phi_g(r)$ corresponds to a rather well-localized 5p orbital on the iodine atom, but the excited state is diffuse, whether it is weakly bound or the continuum itself. For excitation of a diffuse, dipole-bound state, we can approximate the relatively small ground state as a δ -function centered at the iodine atom, in which case the cross-section becomes simply proportional to the value of the electron density in the dipole-bound excited state in the vicinity of the iodine atom (located at position R_I^-):

$$\sigma(h\nu) \propto \phi_f^E(R_I^-)^2 \quad (8)$$

In this picture, a larger dipole moment on M compresses the diffuse, dipole-bound state closer to the core, giving rise to a larger value of the wave function, $\phi_f^E(R_I^-)$, at the position of the iodine atom. As the transition to the dipole bound state grows in intensity, this increase comes at the expense of the integrated cross-section for excitation of the continuum since the total cross-section is constrained by the oscillator strength sum rule.²⁹ We have found a rough correlation between the ratio of the peak absorption to that of the adjoining continuum, $\sigma_{DB}/\sigma_{cont}$, as a function of the dipole moment of the solvent molecule. This trend is displayed in Figure 6, where the filled data symbols are taken from $I^- \cdot M$ monosolvated species while the open symbols correspond to two solvent molecules (with $\mu_{cluster} \equiv 2\mu_{monomer}$), as we will discuss in the next section.

IV. Application to Ternary ($I^- \cdot M_2$) Systems

IVA. Evidence for Asymmetric Ion Solvation. The increasing prominence of the absorption peak with the dipole moment of the solvent molecule (Figure 1) suggests that the electronic absorption envelope of an anion–molecule complex can be used to estimate the dipole moment of the neutral cluster formed upon photodetachment (i.e. at the geometry of the ion). This, in turn, yields a “first-order” description of the anionic cluster structure by constraining the possible relative orientations of the two (or more) solvent molecules contributing to the net dipole. Consider, for example, the simple $I^- \cdot (CH_3CN)_2$ cluster discussed in the Introduction. The solvent molecules may be arranged around the halide ion in two extreme ways, that is, either symmetrically (with the two solvent molecules on opposite sides of the ion) or asymmetrically (with both solvents on the same side of the ion). In earlier work, Hiroaka et al.³⁰ analyzed thermochemical measurements in the context of ab initio calculations (at the HF/3-21G* level) on the symmetric structure, and Markovich et al.⁴ also found the symmetric structure in MD simulations on $I^- \cdot (CH_3CN)_2$. Dipole-bound, excited-state spectroscopy provides a relatively simple check of this assignment since the symmetrical arrangement has no net vertical dipole moment and would not therefore

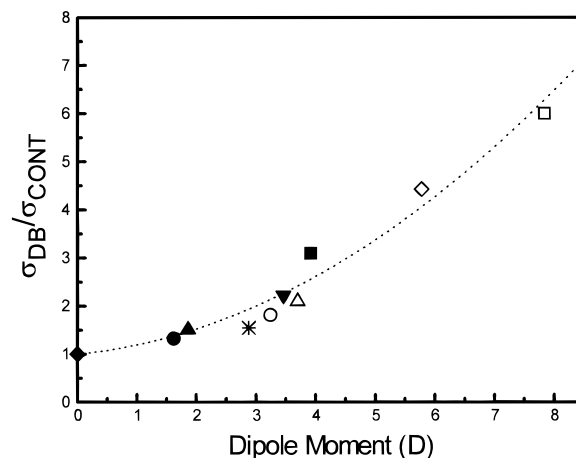


FIGURE 6. Plot of the cross-section for excitation of the dipole-bound state relative to the continuum as a function of the dipole moment of the neutral solvent molecule M. The filled symbols represent $I^- \cdot M$ ion–molecule complexes, while the open symbols correspond to the ternary complexes, $I^- \cdot M_2$, for M: $\blacklozenge = N_2$, $\bullet = CH_3I$, $\blacktriangle = CH_3F$, $* = (CH_3)_2CO$, $\blacktriangledown = CH_3NO_2$, $\blacksquare = CH_3CN$, $\circ = (CH_3I)_2$, $\triangle = (CH_3F)_2$, $\diamond = (CH_3CN \cdot CH_3F)$, and $\square = (CH_3CN)_2$.

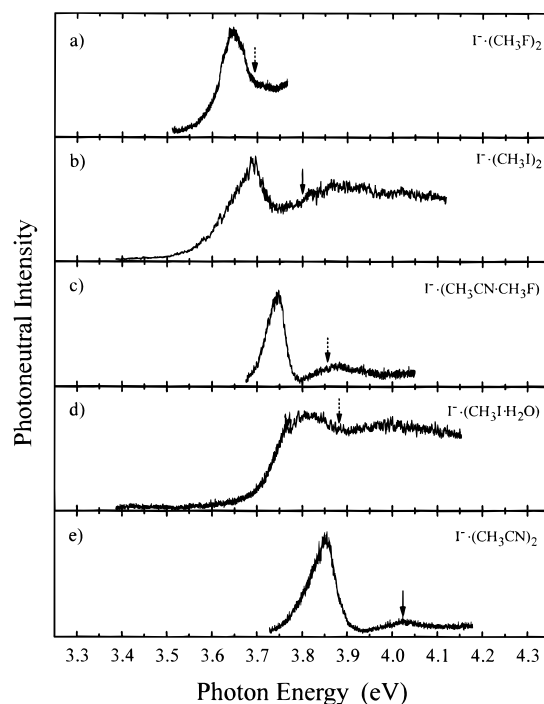


FIGURE 7. Absorption (fast photoneutral action) spectra of mixed and pure ternary complexes, $I^- \cdot M_2$. The solid arrows mark the experimental VDEs of the complexes, while the dashed arrows mark the VDEs calculated from thermochemical data.³¹

support a dipole-bound excited state, while the asymmetric structure has a very large ($2\mu_{CH_3CN} \approx 8$ D) dipole.

Absorption spectra for the series $I^- \cdot M_2$ ($M = CH_3I$, CH_3F , CH_3CN), as well as several mixed variations, are reproduced in Figure 7. The dipole moments of CH_3I , CH_3F , and CH_3CN monomers are 1.62, 1.85, and 3.92 D, respectively. Solvation by methyl fluoride and methyl iodide dimers (upper two traces) yields a clear absorption feature below the detachment continuum, similar to that of the nitromethane monomer (3.46 D), while the spectra

from the mixed $\text{CH}_3\text{F}\cdot\text{CH}_3\text{CN}$ and pure $(\text{CH}_3\text{CN})_2$ clusters are dominated by transitions to excited states located well below their corresponding VDEs. Interestingly, we observed strong absorption maxima for all of the pure and mixed C_{3v} systems, while the mixed cluster with water, $\text{CH}_3\text{I}\cdot\text{H}_2\text{O}$, (Figure 7d) shows very little enhancement, even though the dipole moment of water (1.8 D) is quite close to that of CH_3F . Thus, the occurrence of the peak below the VDE is not simply related to the magnitudes of the solvent molecules' dipole moments but how they are arranged in the cluster.

In the C_{3v} systems, the intense, localized absorption bands below their VDEs strongly suggest that I^- is solvated in the asymmetric, high-dipole moment configuration ($\text{I}^-\cdot\text{M}-\text{M}$) in all three cases. We note that a second, much weaker and broader peak occurs near the VDE in traces b–e in Figure 7. The origin of this peak is unclear; it may correspond to an isomer of the cluster with a considerably smaller vertical dipole moment²⁰ or to the onset of a second dipole-bound excited state of the cluster.^{10,32} As mentioned above, the ratio of bound and continuum cross-sections was included in Figure 6 for the C_{3v} systems, plotted on the assumption that $\mu_{\text{dimer}} \equiv 2\mu_{\text{monomer}}$. There is a smooth trend extending from monomers to pure and mixed dimers, and these absorption spectra represent the first direct evidence for asymmetric anion solvation in the gas phase.³³

IVB. Photochemistry of the Asymmetrically Solvated Ions: Precursors to High-Energy neutral van der Waals Isomers? By analogy with the photochemistry of the $\text{I}^-\cdot\text{M}$ binary complexes presented in section III, photoexcitation of $\text{I}^-\cdot(\text{CH}_3\text{CN})_2$, for example, should again cleave the solvent molecules from the halide to form the dipole-bound anion of the neutral dimer. Figure 8 presents the photofragment mass spectra observed for excitation of three C_{3v} complexes at the peaks of their respective electronic spectra (Figure 7). The $\text{I}^-\cdot(\text{CH}_3\text{F})_2$ system, built upon the monomer with the smallest dipole moment, does not yield anionic fragments (Figure 8a), while the mixed $\text{I}^-\cdot(\text{CH}_3\text{CN}\cdot\text{CH}_3\text{F})$ system decays primarily to the CH_3CN^- anion with a small amount of the binary complex, $(\text{CH}_3\text{CN}\cdot\text{CH}_3\text{F})^-$ (Figure 8b). Excitation of the $\text{I}^-\cdot(\text{CH}_3\text{CN})_2$ complex, on the other hand, creates primarily the $(\text{CH}_3\text{CN})_2^-$ anion (Figure 8c). To establish whether these binary complexes are indeed dipole-bound excess electron systems, we utilize the field detachment scheme described in section III C (see Figures 3 and 4). The results for the acetonitrile dimer anion are shown in Figure 9, indicating that about 80% of these anions are readily stripped of their excess electron, as expected for a dipole-bound system.

Since the $(\text{CH}_3\text{CN})_2^-$ anion contains a diffuse excess electron, we can be sure that the arrangement of the acetonitrile molecules will be largely governed by the neutral force field. We therefore conclude that the anion structure must derive from a stable neutral van der Waals core with a high dipole moment. Spectroscopic studies have confirmed, however, that the only dimeric species isolated upon condensation of acetonitrile (in a free jet)

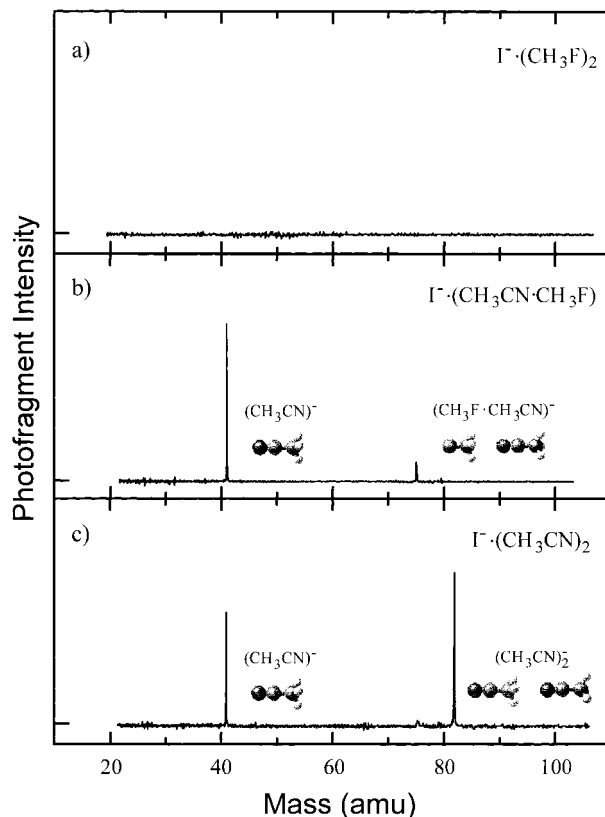


FIGURE 8. Photofragment ion mass spectra from the excitation of (a) $\text{I}^-\cdot(\text{CH}_3\text{F})_2$, (b) $\text{I}^-\cdot(\text{CH}_3\text{CN}\cdot\text{CH}_3\text{F})$, and (c) $\text{I}^-\cdot(\text{CH}_3\text{CN})_2$ complexes at their absorption maxima.

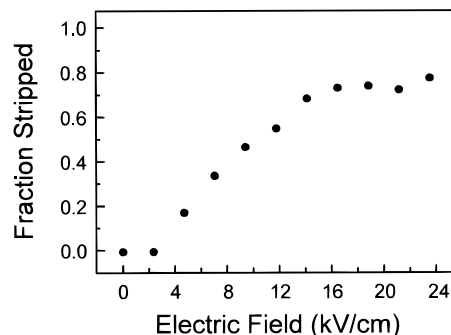


FIGURE 9. Fraction of neutrals produced by field detaching the weakly bound excess electron from the $(\text{CH}_3\text{CN})_2^-$ photofragment using the apparatus displayed in Figure 3.

corresponds to the most stable form where the molecular dipoles align in an antiparallel configuration.^{34,35} Thus, the linear form inferred from the existence of the dipole-bound anion must be a locally stable, high-energy isomer. Interestingly, Bohm³⁶ and Chandler³⁷ showed in their calculations that the local structure of liquid CH_3CN displays the linear binding motif in which two acetonitrile molecules lie parallel to each other, maximizing the number of N–H contacts. In more recent calculations, Wales and co-workers⁵ postulated the existence of a high-energy isomer of the dimer where, like the liquid, the acetonitrile molecules are aligned in this collinear configuration. This high-energy isomer is thought to reside in a shallow well, 0.125 eV above the ground-state complex. While the barrier to interconversion is only

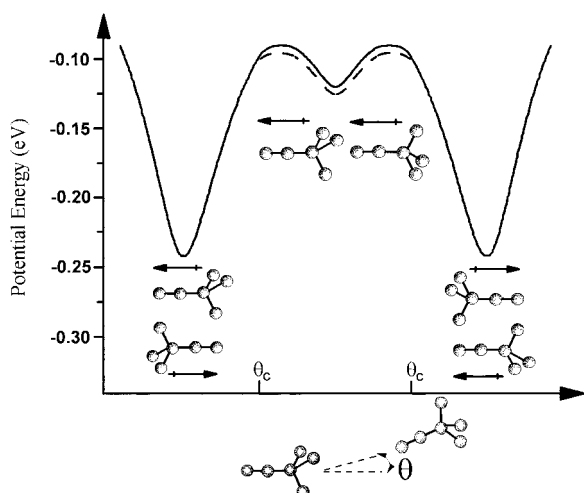


FIGURE 10. Schematic diagram of the potential energy surface of the acetonitrile dimer, plotted as a function of the angle between the axes of the molecules as one is rotated about the other. The dipole-bound anion, formed by electron attachment to the high-energy collinear isomer, is depicted by the dashed line, with θ_c representing the angle at which the anionic surface crosses the neutral surface. The numerical values refer to minima on the neutral surface and are taken from the calculations of Popelier et al.⁵

0.025 eV, it is apparently sufficiently high to support a long-lived isomer before it relaxes back to the antiparallel form. The situation is depicted in Figure 10, where the dotted line indicates the dipole-bound anionic state, which disappears as the two molecules rotate about one another and cancel each other's dipole.

The increasing propensity for formation of the anionic dimers with increasing dipole moments of the constituents (Figure 8) is significant, suggesting that the upper minimum in the potential (Figure 10) becomes more pronounced due to the dipole–dipole interaction. Indeed, the photosynthetic scheme for preparing these species provides a straightforward means with which to explore how such minima evolve as the components of the binary complexes are systematically varied. This application is still in its infancy, but the method is general and should be readily extendable to other (e.g. non- C_{3v} symmetry) classes of solvent molecules.

Returning to the neutral complexes which lie at the core of the diffuse, dipole-bound binary anions, we note that the field detachment technique used to probe for weak electron binding in the $(\text{CH}_3\text{CN})_2^-$ anion (Figure 9) is an ideal method for *preparing the linear neutral van der Waals dimer* once we have the dipole-bound anion. This approach exploits the strong electric field around an atomic ion to overcome the intermolecular potential between two solvent molecules and establish a unique arrangement resulting from the competition between van der Waals and electrostatic forces. Basically, the ion acts as a “template” to enforce a particular relative orientation of the solvent molecules. We then photocleave the oriented complex away from the ion template without causing it to rearrange into a more stable form, provided

that the ion-enforced structure corresponds to a local minimum on the neutral intermolecular potential energy surface.

V. Summary

We have demonstrated that the long-range interaction between a photoejected electron and the cluster core can be used to deduce the arrangement of solvent molecules around halide anions. The spectra reveal that when a second solvent molecule binds to a monosolvated anion, it occupies an asymmetric position (i.e. $X^- \cdot M \cdot M$, with the outer M in the second solvation shell). The neutral frameworks of these asymmetric ionic forms display very large dipole moments, leading to the formation of dipole-bound excited states just below the vertical electron detachment energies of the anions. Asymmetric solvation is generally observed for polar solvent molecules with C_{3v} symmetry. Photoexcitation of the complexes to their dipole-bound excited states releases the solvent from the halogen atom as a ground-state, dipole-bound anion, providing an efficient means for studying these fragile anions. For the $X^- \cdot M_2$ clusters, the solvents are released with retention of the high dipole geometry of the core complex and the excess electron can be field stripped as the final step in an efficient “photosynthetic” route to high-energy isomers of neutral vdW complexes.

We thank the National Science Foundation for support of this work.

References

- (1) Marcus, Y. *Ion Solvation*; Wiley: Chichester, U.K., 1985; p 41.
- (2) Dessent, C. E. H.; Bailey, C. G.; Johnson, M. A. In *Structure and Dynamics of Clusters*; Kondow, T., Kaya, K., Terasaki, A., Eds.; Universal Academy Press: Tokyo, 1996; p 329.
- (3) Dessent, C. E. H.; Kim, J.; Johnson, M. A. *J. Phys. Chem.* **1996**, *100*, 12.
- (4) Markovich, G.; Perera, L.; Berkowitz, M. L.; Cheshnovsky, O. *J. Chem. Phys.* **1996**, *105*, 2675.
- (5) Popelier, P. L. A.; Stone, A. J.; Wales, D. J. *Faraday Discuss.* **1994**, *97*, 243.
- (6) Shimamura, I.; Takayanagi, K. *Electron–Molecule Collisions*; Plenum: New York, 1984; p 382.
- (7) Bailey, C. G.; Dessent, C. E. H.; Johnson, M. A.; Bowen, K. H., Jr. *J. Chem. Phys.* **1996**, 6976.
- (8) Desfrancois, C.; Khelifa, N.; Schermann, J. P. *Phys. Rev. Lett.* **1994**, *73*, 2436.
- (9) Garrett, W. R. *J. Chem. Phys.* **1982**, *77*, 3666.
- (10) Marks, J.; Brauman, J. I.; Mead, R. D.; Lykke, K. R.; Lineberger, W. C. *J. Chem. Phys.* **1988**, *88*, 6785.
- (11) Jortner, J.; Rice, S. A.; Wilson, E. G. *Metal-Ammonia Solutions*; Benjamin: New York, 1964.
- (12) Deng, Z.; Martyna, G. J.; Klein M. L. *J. Chem. Phys.* **1994**, *100*, 7590.
- (13) $\sigma \propto (h\nu - EA)^{l+1/2}$, where l = the angular momentum of the ejected electron and EA = the electron affinity of the molecule, shown by the arrow in Figure 1a.
- (14) Abdoul-Carime, H. Ph.D. Thesis, Laboratoire de Physique de Lasers, Université Paris-Nord, 1996.

- (15) Johnson, M. A.; Lineberger, W. C. In *Technique for the Study of Gas-Phase Ion Molecule Reactions*; Farrar, J. M., Saunders, W., Eds.; Wiley: New York, 1988; p 591.
- (16) The photoelectron spectra (PES) were obtained at 4.66 eV ($\sim 2 \times 10^5$ laser shots of Nd:YAG fourth harmonic) and are calibrated to ± 10 meV.²² In addition to providing the detachment thresholds, photoelectron spectra are useful as they confirm the identity of the clusters as ion-dipole complexes where the excess charge is localized on the halide ion.
- (17) Posey, L. A.; DeLuca, M. J.; Johnson, M. A. *Chem. Phys. Lett.* **1986**, *131*, 170.
- (18) Cyr, D. M.; Scarton, M. G.; Johnson, M. A. *J. Chem. Phys.* **1993**, *99*, 4869.
- (19) Dessent, C. E. H.; Bailey, C. G.; Johnson, M. A. *J. Chem. Phys.* **1995**, *102*, 6335.
- (20) Dessent, C. E. H.; Bailey, C. G.; Johnson, M. A. *J. Chem. Phys.* **1995**, *103*, 2006.
- (21) Bailey, C. G. *Private communication*.
- (22) Arnold, C. C.; Neumark, D. M.; Cyr, D. M.; Johnson, M. A. *J. Phys. Chem.* **1995**, *99*, 1633.
- (23) Desfrancois, C.; Abdoul-Carime, H.; Adjouri, C.; Khelifa, N.; Schermann, J. P. *Europhys. Lett.* **1994**, *26*, 25.
- (24) Popple, R. A.; Finch, C. D.; Dunning, F. B. *Chem. Phys. Lett.* **1995**, *234*, 172.
- (25) Latimer, C. J. *Contemp. Phys.* **1979**, *20*, 631.
- (26) Zhao, Y.; Yourshaw, I.; Reiser, G.; Arnold, C. C.; Neumark, D. M. *J. Chem. Phys.* **1994**, *101*, 6538.
- (27) This effect has been observed previously in the study of the interaction of a gas with positive electron affinity on high Rydberg states of atoms. Basically, a bare iodine atom cannot accept the electron while conserving both energy and momentum, similar to the fact that isolated electrons cannot absorb a photon.
- (28) Stockdale, J. A.; Davis, F. J.; Compton, R. N.; Klots, C. E. *J. Chem. Phys.* **1974**, *60*, 4279.
- (29) Fano, U.; Cooper, J. W. *Phys. Rev.* **1965**, *137*, 1364.
- (30) Hiraoka, K.; Mizuse, S.; Yamabe, S. *J. Phys. Chem.* **1988**, *92*, 3943.
- (31) Glukhovtsev, M. N.; Pross, A.; Radom, L. *J. Am. Chem. Soc.* **1996**, *118*, 6273.
- (32) Clary, D. C.; Henshaw, J. P. *Int. J. Mass Spectrom. Ion Processes* **1987**, *80*, 31.
- (33) Perera, L.; Berkowitz, M. L. *J. Chem. Phys.* **1991**, *95*, 1954.
- (34) Knozinger, E.; Leutloff, D. *J. Chem. Phys.* **1984**, *74*, 4812.
- (35) Buck, U.; Gu, X. J.; Krohne, R.; Laurenstein, Ch. *Chem. Phys. Lett.* **1990**, *174*, 247.
- (36) Bohm, H. J.; McDonald, I. R.; Madden, P. A. *Mol. Phys.* **1983**, *49*, 347.
- (37) Hsu, C. S.; Chandler, D. *Mol. Phys.* **1978**, *36*, 215.

AR950061F